

## Rapid Synthesis of Mesoporous SBA-16 Silica in Weakly Acidic Media

Hua Wang,<sup>\*1</sup> Caiyun Han,<sup>2</sup> Hongping Pu,<sup>2</sup>  
Liuyi Zhang,<sup>2</sup> Zhaohua Zou,<sup>2</sup>  
and Yongming Luo<sup>\*1,2</sup>

<sup>1</sup>Faculty of Materials and Metallurgical Engineering,  
Kunming University of Science and Technology,  
Kunming 650093, P. R. China

<sup>2</sup>Faculty of Environmental Science and Engineering,  
Kunming University of Science and Technology,  
Kunming 650093, P. R. China

Received September 17, 2009

E-mail: luoyongming@tsinghua.org.cn

Well-ordered mesoporous SBA-16 (with *Im3m* symmetry) has been synthesized within 6 h in weakly acidic media in the presence of phosphomolybdic acid and inorganic salts. The aforementioned materials were characterized by XRD, N<sub>2</sub> adsorption–desorption, and TG-DTA.

Since the discovery of the (OMSMs) M41S family of ordered mesoporous silica materials, explosive research in this area has opened new vistas in materials science, and a wide variety of OMSMs such as SBA, MSU, FDU, JLU, FSM, and KIT have been synthesized with cationic, anionic, neutral, and nonionic surfactants through various assembly routes. Among them, mesoporous SBA-16 has attracted a lot of attention for potential applications in adsorption, catalysis, and separation as well as in immobilization of biomolecules and catalysts because of its 3D channel systems and uniform-sized pores of superlarge cage-like structures,<sup>1,2</sup> which are less susceptible to pore blockage and is favorable for the transport of reactants and products.<sup>3</sup> It is well-known that SBA-16 has been synthesized mostly by using nonionic triblock copolymer F127 (or F108) as a structure directing agent under strongly acidic conditions (pH < 1), which might be expected to proceed through a (S<sup>0</sup>H<sup>+</sup>) (X<sup>−</sup>I<sup>+</sup>) pathway.<sup>1,4</sup> It is obvious that such a strongly acidic medium is disadvantageous for the industrialization of ordered SBA-16 due to practical problems such as erosion of reaction vessels, harm to workers, and environmental problems. Weakly acidic media is however especially prone to the formation of amorphous or otherwise disordered silica because of the absence of sufficiently strong electrostatic or hydrogen-bonding interactions.<sup>5</sup> On the other hand, it is well-known that most molecular sieves are synthesized by hydrothermal methods, which generally suffer from the drawback of long crystallization (aging) time.<sup>6</sup> Moreover, the corresponding aging time required for synthesis of OMSMs with triblock copolymer templates would be obviously increased if the molar ratio of

HCl to Si is lower than 0.59.<sup>7</sup> Although the aging time for microwave synthesis of SBA-16 can be shortened to within 2 h, the molar ratio of HCl to Si is as high as 6.68.<sup>8</sup>

Of late, limited synthesis efforts have been made to obtain SBA-16 in weakly acidic media, which includes adding cationic fluorocarbon surfactant,<sup>9</sup> using a two-step route<sup>10</sup> and using ternary surfactants.<sup>11,12</sup> Despite significant progress in the synthesis of SBA-16, further studies in this area are desirable, especially in relation to their thermal and hydrothermal stability. In our previous work, we synthesized SBA-15 in low-concentration HCl media.<sup>13</sup> However, as the synthesis of mesoporous SBA-16 is affected by many factors (e.g., temperature, stirring), it is much more difficult to synthesize SBA-16 than SBA-15 under weakly acidic conditions.<sup>10,11</sup>

In this article, we report a facile and rapid route for the synthesis of mesoporous SBA-16 under weak acidic conditions, with the molar ratio of HCl to Si as low as 0.21. F127 was employed as a template, following a previous procedure for synthesis of SBA-15<sup>13</sup> except for the addition of a small amount of inorganic salt, the modifications of the starting chemical composition, and reaction temperature. In a typical batch, 2.4 g of F127 was dissolved in 72 g of distilled water with vigorous stirring at room temperature (RT), then 0.23 g of phosphomolybdic acid (H<sub>3</sub>PO<sub>4</sub>·12MoO<sub>3</sub>·24H<sub>2</sub>O, abbreviated to HPMo) was added to the solution to keep the molar ratio of Si/Mo = 20.0. After F127 and HPMo were dissolved completely, 5.08 g of TEOS, 0.35 g of NaCl, and 0.45 mL of c-HCl (*w* = 36%) were added to the above mixture. The resulting mixture of the following molar composition: 1TEOS: 0.0079F127:0.0042HPMo:0.25NaCl:0.21HCl:166.67H<sub>2</sub>O was stirred for 20 h at RT and subsequently aged at 100 °C overnight without stirring. Finally, the reaction products were filtered, washed, dried, and calcined at 550 °C in air for 8 h.

The N<sub>2</sub> adsorption–desorption isotherm of the sample is type IV, and a H<sub>2</sub>-type hysteresis loop starting at a relative pressure of 0.6–0.7 and abruptly ending at 0.45 is also distinctly observed (Figure 1), indicating the presence of good quality cage-like pores.<sup>14</sup> BJH pore size distribution curves of the sample are presented in Figure S1 (see ESI), and the entrance size and the cage size calculated from the desorption and the adsorption branch are about 3.6 and 6.8 nm, respectively. The XRD pattern of sample 5 exhibits three well-resolved diffraction peaks (Figure 1, insert) that can be easily indexed as (110), (200), and (211) reflections, corresponding to a *Im3m* cubic structure, as confirmed by TEM and the corresponding FFT pattern (Figure S2 in ESI). The cell parameters, BET surface area and the total pore volume of the sample are 16.6 nm, 776 m<sup>2</sup> g<sup>−1</sup>, and 0.9 cm<sup>3</sup> g<sup>−1</sup>, which is comparable to those of sample S-4 prepared with a conventional synthesis route (see ESI). In addition, other inorganic salts such as KCl, Na<sub>2</sub>SO<sub>4</sub>, and K<sub>2</sub>SO<sub>4</sub> can also be used to synthesize ordered SBA-16 in weakly acidic media.

Thermogravimetry and differential thermal analysis (TG-DTA) of as-synthesized sample 5 were conducted and the corresponding results are displayed in Figure 2. It is clear that the sample exhibited a total weight loss of about 31% in the temperature range of 50 to 800 °C with maximum loss occurring at about 280 °C. It is notable that a three-step profile is also observed, which can be explained as follows. The first

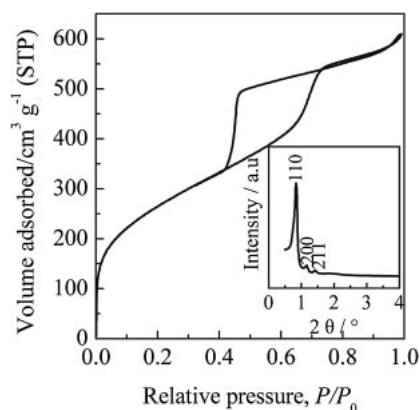


**Figure 1.** N<sub>2</sub> adsorption-desorption isotherms and XRD pattern (insert) of sample 5.

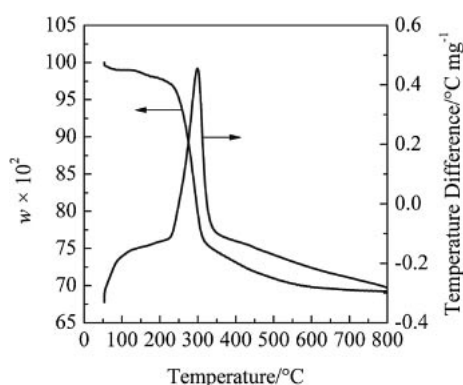


**Figure 2.** Thermogravimetry and differential thermal analysis TG-DTA curve of sample 5.

step with 2% weight loss in the range of 50–180 °C can be attributed to the desorption of adsorbed water. 25% TGA weight loss with an exothermic DTA peak in the second step at temperatures ranging from 180 to 400 °C is due to the decomposition and combustion of the triblock polymeric surfactant F127. The third step (about 3% weight loss) in the region of 400–650 °C could be ascribed to the release of water arising from the condensation and polymerization of the silanol groups within the framework of mesoporous silica.

Figure 3 provides the corresponding XRD patterns of the samples synthesized with various crystallization time, and the physicochemical properties such as total pore volume, BET specific surface area, and unit cell parameter of the samples are summarized in Table 1. Noticeably, three well-resolved peaks in the region of 0.8–1.5°, indexed to the (110), (200), and (211) reflections, are detected for the samples with age time more than 3 h, which could be associated with the body-centered cubic space group (*Im3m*). The results indicate that the highly ordered mesoporous SBA-16 could be synthesized within 6 h in such low concentration HCl media, which is very short compared to the aging time required for other synthesis methods (i.e., 1–3 days).<sup>1,10–12</sup> As can be seen by comparing Table 1, it is worth noting that there is a noticeable increase in unit cell parameter ( $a_0$ ), pore diameter, total and mesoporous pore volume with increased aging time. It is well-documented that (EO)<sub>*m*</sub>(PO)<sub>*n*</sub>-(EO)<sub>*m*</sub> triblock copolymers in water form micelles, where the (PO)<sub>*n*</sub> moieties of the surfactant exhibit stronger hydrophobicity

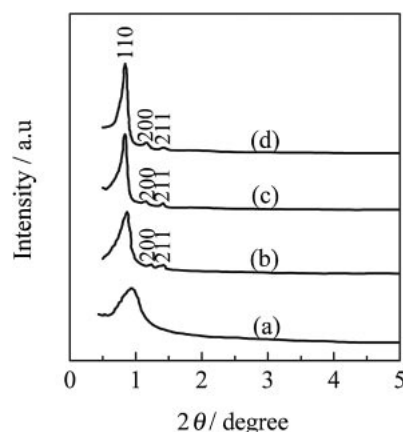


**Figure 3.** XRD patterns of (a) sample 2, (b) sample 3, (c) sample 4, and (d) sample 5.

than the (EO)<sub>*m*</sub> moieties.<sup>15a</sup> Moreover, the hydrophobicity of the (EO)<sub>*m*</sub> moieties increases with temperature.<sup>15b,15c</sup> The long crystallization time is expected to be in favor of the hydrophobicity of the (EO)<sub>*m*</sub> moieties, thus resulting in the hydrophobic domain volumes and the length of (PO)<sub>*n*</sub> moieties increasing, which corresponds to the reduction of the hydrophilic domain volumes and the occlusion of the PEO moieties in the matrix, which are responsible for  $d_{110}$  spacing, pore size, and pore volume increase. On the other hand, the addition of inorganic salts has the same effect as the increase in temperature.<sup>15d</sup> Analogous phenomenon was observed for synthesis of SBA-15.<sup>13,16</sup>

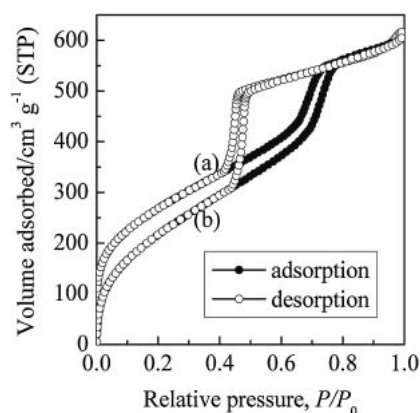
By using the same surfactant but without adding HPMo in weak acidic media, the product sample S-1 is disordered, which is supported by XRD and N<sub>2</sub> adsorption-desorption characterization results as shown in Table S1 and Figure S3, respectively (see ESI). This is believed to be related to the absence of sufficiently strong electrostatic or hydrogen-bonding interactions in the synthesis medium.<sup>5,13,17</sup> Moreover, the results of N<sub>2</sub> adsorption-desorption and XRD show the sample S-2 synthesized without adding inorganic salts is also disordered (see ESI). It is well-documented that inorganic salts play a crucial role in the synthesis of ordered mesoporous silica materials.<sup>18,19</sup> Therefore, the most likely explanation for the structure difference observed here is that the addition of inorganic salts can increase the interaction of silicate species with hydrophilic moieties of nonionic block copolymers. The strong interaction can result in long-range ordered domain of silica-surfactant mesostructure and favor the formation of ordered mesoporous silica material.

Figure 4 illustrates N<sub>2</sub> adsorption-desorption isotherms of sample 5 before and after treatment with 100 °C water for 120 h (sample 5 and sample 6). Clearly, a type IV isotherm taken together with a typical H<sub>2</sub> hysteresis loop is still detected for sample 6, while the jumps of the adsorption and desorption branch shift slightly to higher relative pressure, indicating both the entrance and the cage size of the sample increase. Compared with sample 5, sample 6 maintains more than 81% of its surface and more than 100% of its pore volume. XRD shows that the sample retains ordered cubic mesostructure after treated with 100 °C water for 120 h (pattern not shown). In contrast, sample S-5 under the same hydrothermal treatment only maintains 43% surface area and 66% pore volume of sam-

**Table 1.** Physicochemical Properties of Mesoporous Silica Synthesized under Weakly Acidic Conditions

| Sample          | HCl/Si <sup>a)</sup> | Si/Mo <sup>a)</sup> | Na/Si <sup>a)</sup> | AT <sup>b)</sup><br>/h | $a_0^c)$<br>/nm | $S_{\text{BET}}^d)$<br>/m <sup>2</sup> g <sup>-1</sup> | TPV <sup>d)</sup><br>/cm <sup>3</sup> g <sup>-1</sup> | MPV <sup>e)</sup><br>/cm <sup>3</sup> g <sup>-1</sup> | Pore diameter/nm  |                   | CS <sup>h)</sup> |
|-----------------|----------------------|---------------------|---------------------|------------------------|-----------------|--|---|---|-------------------|-------------------|------------------|
|                 |                      |                     |                     |                        |                 |  |   |   | CSD <sup>f)</sup> | ESD <sup>g)</sup> |                  |
| 1               | 0.21                 | 20.0                | 0.25                | 0                      | —               | 626  | 0.73  | 0.49  | —                 | —                 | disordered       |
| 2               | 0.21                 | 20.0                | 0.25                | 3                      | —               | 651  | 0.76  | 0.52  | —                 | —                 | disordered       |
| 3               | 0.21                 | 20.0                | 0.25                | 6                      | 16.1            | 713  | 0.82  | 0.59  | 6.5               | 3.3               | cubic            |
| 4               | 0.21                 | 20.0                | 0.25                | 12                     | 16.4            | 745  | 0.86  | 0.64  | 6.7               | 3.5               | cubic            |
| 5               | 0.21                 | 20.0                | 0.25                | 24                     | 16.6            | 776  | 0.90  | 0.69  | 6.9               | 3.6               | cubic            |
| 6 <sup>i)</sup> | —                    | —                   | —                   | —                      | 16.5            | 629  | 0.91  | 0.72  | 7.5               | 4.0               | cubic            |

a) Molar ratio. b) AT: age time. c) Unit cell parameter  $a_0 = d_{110} \times \sqrt{2}$ . d) TPV: the total pore volume. e) MPV: mesoporous pore volume. f) The cage size distribution calculated from the adsorption branch. g) The entrance size distribution calculated from desorption branch. h) CS: crystal structure was characterized by XRD. i) The sample 5 was treated with 100 °C water for 120 h.

**Figure 4.** N<sub>2</sub> adsorption-desorption isotherms of sample 5 before and after hydrothermal stability test: (a) before and (b) after treating with 100 °C water for 120 h.

ple S-4 (see ESI), respectively. The high hydrothermal stability of sample 5 might be ascribed to the higher degree of polymerization and condensation of silanol groups, which originated from the synergistic effect of rapid nucleation with the aid of HPMo<sup>13</sup> and salt effect<sup>20</sup> during crystallization.

In conclusion, we have developed a facile and rapid route for synthesis of mesoporous SBA-16 with well-ordered *Im3m* cubic structure. The high hydrothermal stability of reaction products might be attributed to the higher degree of polymerization and condensation of silanol groups, which arisen from the synergistic effect of rapid nucleation with the aid of HPMo and salt effect during the aging process.

This work was supported by the National Natural Science Foundation of China (Nos. 20867003, 90610035, and 50774038), Young Academic and Technical Leader Raising Foundation of Yunnan Province (No. 2008py010), and Natural Science Foundation of Kunming University of Science and Technology (No. KKZ3200822027), Key Program of Natural Science Foundation of Yunnan Province (No. 2007E0014Z).

### Supporting Information

Figure S1 (BJH pore size distribution), Figure S2 (TEM and FFT), Figure S3 (N<sub>2</sub> adsorption-desorption isotherms), and Table S1 are presented in Supporting Information. This material is available free of charge on the web at <http://www.csj.jp/journals/bcsj/>.

### References

- 1 D. Y. Zhao, Q. S. Huo, J. L. Feng, B. F. Chmelka, G. D. Stucky, *J. Am. Chem. Soc.* **1998**, *120*, 6024.
- 2 Y. Sakamoto, M. Kaneda, O. Terasaki, D. Y. Zhao, J. M. Kim, G. Stucky, H. J. Shin, R. Ryoo, *Nature* **2000**, *408*, 449.
- 3 R. M. Grudzien, B. E. Grabicka, M. Jaroniec, *J. Mater. Chem.* **2006**, *16*, 819.
- 4 a) X. Meng, D. Lu, T. Tatsumi, *Microporous Mesoporous Mater.* **2007**, *105*, 15. b) W. J. J. Stevens, M. Mertens, S. Mullens, I. Thijs, G. V. Tendeloo, P. Cool, E. F. Vansant, *Microporous Mesoporous Mater.* **2006**, *93*, 119.
- 5 D. Y. Zhao, J. L. Feng, Q. S. Huo, N. Melosh, G. H. Fredrickson, B. F. Chmelka, G. D. Stucky, *Science* **1998**, *279*, 548.
- 6 R. Kumar, A. Bhaumik, R. K. Ahedi, S. Ganapathy, *Nature* **1996**, *381*, 298.
- 7 P. Schmidt-Winkel, P. D. Yang, D. I. Margolese, B. F. Chmelka, G. D. Stucky, *Adv. Mater.* **1999**, *11*, 303.
- 8 Y. K. Hwang, J.-S. Chang, Y.-U. Kwon, S.-E. Park, *Microporous Mesoporous Mater.* **2004**, *68*, 21.
- 9 Y. Han, J. Y. Ying, *Angew. Chem., Int. Ed.* **2005**, *44*, 288.
- 10 Z. W. Jin, X. D. Wang, X. G. Cui, *J. Colloid Interface Sci.* **2007**, *307*, 158.
- 11 B.-C. Chen, M.-C. Chao, H.-P. Lin, C.-Y. Mou, *Microporous Mesoporous Mater.* **2005**, *81*, 241.
- 12 C.-L. Lin, Y.-S. Pang, M.-C. Chao, B.-C. Chen, H.-P. Lin, C.-Y. Tang, C.-Y. Lin, *J. Phys. Chem. Solids* **2008**, *69*, 415.
- 13 Y. M. Luo, Z. Y. Hou, R. T. Li, X. M. Zheng, *Microporous Mesoporous Mater.* **2008**, *109*, 585.
- 14 a) J. R. Matos, M. Kruk, L. P. Mercuri, M. Jaroniec, L. Zhao, T. Kamiyama, O. Terasaki, T. J. Pinnavaia, Y. Liu, *J. Am. Chem. Soc.* **2003**, *125*, 821. b) R. M. Grudzien, B. E. Grabicka, M. Jaroniec, *Appl. Surf. Sci.* **2007**, *253*, 5660.
- 15 a) M. Imp  rator-Clerc, P. Davidson, A. Davidson, *J. Am. Chem. Soc.* **2000**, *122*, 11925. b) M. Kruk, M. Jaroniec, C. H. Ko, R. Ryoo, *Chem. Mater.* **2000**, *12*, 1961. c) G. Wanka, H. Hoffmann, W. Ulbricht, *Macromolecules* **1994**, *27*, 4145. d) P. R. Desai, N. J. Jain, R. K. Sharma, P. Bahadur, *Colloids Surf., A* **2001**, *178*, 57.
- 16 B. L. Newalkar, S. Komarneni, H. Katsuki, *Chem. Commun.* **2000**, 2389.
- 17 S. A. Bagshaw, E. Prouzet, T. J. Pinnavaia, *Science* **1995**, *269*, 1242.
- 18 W. Z. Zhang, B. Glomski, T. R. Pauly, T. J. Pinnavaia, *Chem. Commun.* **1999**, 1803.
- 19 a) C. Z. Yu, B. Z. Tian, J. Fan, G. D. Stucky, D. Y. Zhao, *J. Am. Chem. Soc.* **2002**, *124*, 4556. b) C. Z. Yu, B. Z. Tian, J. Fan, G. D. Stucky, D. Y. Zhao, *Chem. Commun.* **2001**, 2726.
- 20 R. Ryoo, S. Jun, *J. Phys. Chem. B* **1997**, *101*, 317.